

Soil-Water Characteristic Curve analysis of silt clay in the Garinono Formation, Sabah

Suleiman Haji Nissor, Siti Jahara Matlan[#], Nazaruddin Abd Taha

Civil Engineering Programme, Faculty of Engineering, Universiti Malaysia Sabah, Jalan UMS, 88400 Kota Kinabalu, Sabah, MALAYSIA.
[#]Corresponding author. E-Mail: jahara@ums.edu.my; Tel: +6013-7762612. Fax: +6088-435324.

ABSTRACT The Soil-Water Characteristic Curve (SWCC) serves as a fundamental tool for investigating unsaturated soils and comprehending the relationship between soil water content and properties. This study analyses the SWCC for silt clay soil from the Garinono Formation in Sandakan, Sabah. Field sampling and laboratory tests were conducted to gather the soil's physical properties and SWCC data, representing the study area. The primary findings illuminate the unsaturated behaviour of the soil within this formation, providing valuable insights into its water retention capabilities. Through rigorous laboratory testing, the SWCC data reveal how the volumetric water content (VWC) changes concerning varying suction conditions (matric potential). The analysis indicates that the SWCC measured data are best represented by Fredlund and Xing model, encompassing the entire range of suction from lower to higher values. The findings underscore significant variations in the SWCC shape based on the bulk density of the soil samples, a crucial indicator of mechanical properties such as compaction and strength. Additionally, the study discusses the direct impact of soil composition and porosity on the SWCC, deepening understanding of their interrelationships. The study's outcomes hold implications for diverse fields, including geotechnical engineering, agriculture, soil science, and environmental science.

KEYWORDS: Soil water characteristic curve; SWCC; Bulk density; Silt Clay; Garinono Formation, Sabah.

Received 7 November 2023 Revised 29 March 2024 Accepted 5 April 2024 Online 10 April 2024 Updated 19 April 2024

© Transactions on Science and Technology

Original Article

INTRODUCTION

The Soil-Water Characteristic Curve (SWCC) is a fundamental soil property in the field of unsaturated residual soil mechanics, serving as a crucial predictor for additional soil attributes, particularly the permeability function (Kristo *et al.*, 2019). The describes the hydromechanical behavior of unsaturated soil and its capacity to retain water relative to matric suction (Luan & Han, 2022). In engineering practices, estimates of unsaturated soil property functions are often derived from the SWCC (Azmi *et al.*, 2019), which proves essential for analyzing issues such as unsaturated soil seepage, stability, and volume changes (Ellithy, 2017). Moreover, geotechnical researchers utilize the soil-water retention curve to assess unsaturated soil parameters including shear strength, permeability coefficient, bearing capacity, and elasticity modules (Mancuso *et al.*, 2012).

The SWCC can be determined directly or indirectly using pedotransfer functions (PTF) and regular soil parameters such as grain-size distribution (GSD), index properties, dry density, and void ratio (Zou & Leong, 2019). Direct laboratory testing of SWCC is expensive and time-consuming due to the low permeability of unsaturated soils, especially at high matric suction values. As a result, researchers have developed empirical models for SWCC. According to Zhang *et al.* (2018) analytical equations, including those proposed by Brooks & Corey (1964), Gardner (1958), van Genuchten (1980), Mualem (1976), McKee & Bumb (1984), and Fredlund & Xing (1994), have been successfully describe the soil-water characteristic curve (SWCC).

Leong & Rahardjo (1997) identified that soil type, mineral concentration, and pore architecture as factors influencing model success. Moreover, Cornelis *et al.* (2005) demonstrated that increasing clay percentage enhances model performance, while higher sand content diminishes it. Bello Yamusa *et al.* (2019) observed that the van Genuchten (1980) and Fredlund & Xing (1994) models provide a good fit for the most of soil water retention curves, particularly with respect to pore-size distributions.

Similarly, Fashi *et al.* (2016) asserted that the van Genuchten (1980) model accurately characterizes water retention in clay loam soil. Conversely, Matlan *et al.* (2014b) concluded that the Brooks & Corey (1964) model performs optimally in representing SWCC for sandy soils, whereas Okovido & Obroku (2021) found it to be most effective for tropical red earth soils.

The Garinono Formation is a chaotic mixture of mud-matrix olistostromes, fractured formations, and tuffaceous strata (Khor *et al.*, 2015). Most of the Garinono Formation consists of slump breccia, with phases of interbedded mudstone, tuff, tuffite, and minor sandstone, and calcinate, forming low hills with moderate slopes (Roslee, 2018; John, 2020). During the wet season, the Garinono Formation becomes expansive soil, swells, and shrinks frequently, causing stability issues in some matrices (John, 2020).

This study aims to analyze SWCC and compare different SWCC model functions, such as those proposed by Brooks & Corey (1964), van Genuchten (1980), Fredlund & Xing (1994), and Kosugi (1994), to determine the most appropriate model for characterizing the SWCC of soil derived from the Garinono Formation. Additionally, the study aims to analyze bulk density's effect on the Garinono Formation's SWCC behavior. Understanding the unsaturated responses and their variations in volumetric water content (VWC) holds crucial implications for stability analysis, engineering design, soil management, and environmental science.

METHODOLOGY

Sample Collection and Testing Approach

The study's methodology encompassed both field sampling and laboratory testing. Fieldwork involved drilling boreholes and collecting disturbed and undisturbed soil samples using sampling tubes with a diameter of 63.5 mm. Samples were collected at depths ranging from 1.5 m to 12.0 m below the ground surface. This investigation took place within the Garinono Formation, an area known for its susceptibility to slope instability due to recurrent mass movements, as documented by Musta *et al.* (2019). The study site is geographically situated at 5.7521° N, 117.7916° E (5° 44' 22.1352" N, 117° 48' 30.8304" E), denoted as "P" in Figure 1, approximately 56.7 km from Sandakan town.

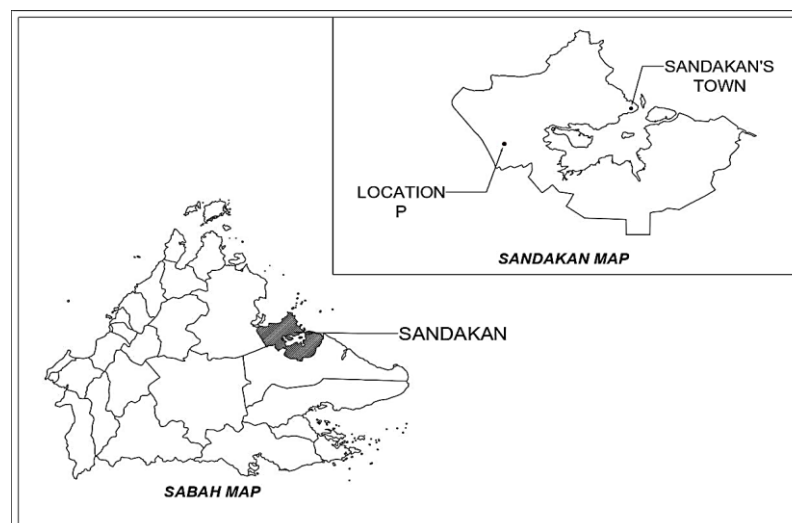


Figure 1. Study location in the Garinono Formation Sandakan, Sabah.

In the laboratory, the disturbed soil samples were subjected to classification tests, which included assessments of particle size distributions, Atterberg limits, field dry densities, natural moisture

contents, and specific gravity. The testing followed the standards outlined in BS 1377: Part 2 and the British Soil Classification System (European Standard, 1997). Additionally, undisturbed soil samples were used to determine the soil-water characteristic of the soil.

Soil Water Characteristic Curve (SWCC) Measurement

The SWCC measurements were conducted in the laboratory using a pressure plate extractor, a reliable method for assessing the SWCC behavior of both coarse and fine-grained soils' bulk density (BD or ρ_b) (Azmi et al., 2019; Sharratt, 1990). Undisturbed samples obtained from 1.5 m below ground level were utilized to measure volumetric water content. The pressure plate extractor recorded suction pressure ranging from 1 to 1,500 kPa. Notably, Fondjo & Dzogbewu (2020) observed that compacted heaving soils typically require suction levels ranging from 671.89 to 2021.8 kPa for optimal moisture conditions.

Undisturbed soil samples were collected at three different depths: (i) at 1.5–2.0 m, (ii) at 2.0–2.5 m, and (iii) at 3.0–3.5 m. The SWCC testing was conducted using a pressure plate extractor apparatus, focusing on samples i, ii, and iii. To prepare the samples for SWCC testing, undisturbed samples were extracted from the tube sampler. A 0.05 m in diameter and 0.05 m in height core ring was driven into the soil using a hammer until it was filled with soil. Subsequently, the core ring was removed, and any excess soil around it was carefully trimmed. The collected samples were securely covered and transported to the laboratory for testing.

The SWCC was determined following the ASTM D6836-02 standard for the Determination of Soil Water Characteristic Curve using a Pressure Extractor. The experiment utilized two pressure chambers (5 bar and 10 bar), a 20-bar air compressor, and saturated ceramic plates. After the samples had been saturated for 24 hours, they were placed on the saturated ceramic plate. The ceramic plate was connected to the water tube for controlled water drainage while the samples were under pressure. Subsequently, the chamber's lid was closed, and pressure was applied to both the chamber and the samples. The samples were pressurized until an equilibrium state was reached, which was indicated when the outflow of water from the chamber ceased. Following this, the compressor was shut off, and the pressure from the chamber and compressor was released. The samples were then weighed to distinguish the differences in water retention before and after pressure was applied. After the final pressure application, the samples were oven-dried for 24 hours and weighed again. In this test, the range of pressure applied to the samples ranged from 0 to 15 bar.

The specimens were weighed to determine their dry mass, allowing for the calculation of gravimetric water content (Equation 2). Equation (1) was employed to compute the soil sample's volumetric water content, θ which was then used to establish the SWCC by linking volumetric water content to matric suction.

Volumetric water content:

$$\theta = \frac{w}{100} \times \rho_b \quad (1)$$

where, ρ_b represents the bulk density, which is the mass of dry soil per unit volume. The variable w corresponds to gravimetric water content, calculated using Equation 2.

$$w = \frac{W_a - W_b}{W_b} \times 100 \% \quad (2)$$

where, W_a is the weight of the moisture sample, and W_b is the weight of the dried sample.

Empirical Models of Soil Water Characteristic Curve (SWCC)

Fitting empirical models to SWCC data helps identify the most appropriate model for representing the soil-water characteristic curve in the Garinono Formation, providing valuable insights into soil-water relationships. Therefore, four empirical models, namely Brooks & Corey (1964), van Genuchten (1980), Fredlund & Xing (1994), and Kosugi (1994), were employed, as these models are prominent and widely cited in the literature.

In general, the normalized water content, Θ also referred to as effective saturation, S_e is commonly used to represent the equations associated with soil-water characteristic curve models. Consider the following equation (Equation 3).

$$\Theta = \frac{\theta - \theta_r}{\theta_s - \theta_r} \text{ (which is dimensionless)} \quad (3)$$

where, θ is volumetric water content ($\text{cm}^3\text{cm}^{-3}$), θ_s is a saturated volumetric water content ($\text{cm}^3\text{cm}^{-3}$) and, θ_r is a residual volumetric water content ($\text{cm}^3\text{cm}^{-3}$).

Brooks & Corey (1964) (BC) Model

One of the pioneering equations for SWCC modeling is the Brooks & Corey (1964), model, which is commonly employed in power-law relationships (Matlan *et al.*, 2014a). The Brooks & Corey (1964) model divides the SWCC into two zones: one where soil suctions are less than the air-entry value and another where they are higher (Fredlund *et al.*, 2011). Equation (4) consists of two equations to represent these zones.

Normalized water content is given by

$$\begin{cases} \Theta = \left[\frac{\psi}{h_b}\right]^{-\lambda} & \psi > h_b \\ \Theta = 1 & \psi \leq h_b \end{cases} \quad (4)$$

where the parameter, h_b is related to the air entry value of the soil, the λ parameter is the pore size index and is related to the pore size distribution of the soil. The Brooks & Corey (1964) model presented by Equation (4) could not calculate soil suction before air input (Fredlund *et al.*, 2011).

The volumetric water content form of the Brooks & Corey (1994) model shown in Equation (5) can be written as follows by substituting Equation (3) into (4).

Volumetric water content is written as

$$\theta = \theta_r + (\theta_s - \theta_r) \left[\frac{\psi}{h_b}\right]^{-\lambda} \quad (5)$$

van Genuchten (1980) (VG) Model

The van Genuchten (1980) model is widely regarded as one of the most advanced models due to its incorporation of fitting parameters. The continuous output of the unsaturated zone generally aligns with the soil-water characteristic curve (Matlan *et al.*, 2014a). Equation (6) presents the van Genuchten's model.

Volumetric water content:

$$\theta = \theta_r + \frac{\theta_s - \theta_r}{[1 + (\alpha\psi)^n]^m} \quad (6)$$

where, ψ is matric suction (kPa), α is scale parameter related to the inverse of air entry value m^{-1} , n is shape parameter related to the pore size distribution of the soil, m is a parameter related to the asymmetry of the model ($m = 1 - 1/n$).

Fredlund & Xing (1994) (FX) Model

Fredlund & Xing (1994) divide the SWCC into three stages: the boundary-effect zone, where pore water is tensioned despite saturated soil. Second, the air replaces water in pore-space desaturation. The third ends with residual water; the ultimate residual saturation zone retains water in soil particles and evaporates (Fattah *et al.*, 2018). Equation (7) presents the Fredlund & Xing's model.

Volumetric water content:

$$\theta = \theta_r + \frac{\theta_s - \theta_r}{\{ \ln[e + (\alpha\psi)^n] \}^m} \quad (7)$$

where, e is the Euler number, an irrational constant equal to 2.71828 in natural logarithm.

Kosugi (1994) (LN) Model

Kosugi (1994) model parameters were developed using a log-normal distribution law (LN) closely connected to soil pore radius distribution (Matlan *et al.*, 2014a). Equation (8) represents Kosugi's log-normal distribution model.

Normalized water content:

$$\Theta = Q \left[\frac{\ln\psi/h_m}{\sigma} \right] \quad (8)$$

where; Q is related to the complementary error function, $\text{erfc}(x)$, and defined in Equation (9).

$$Q(x) = \text{erfc} \left(\frac{x/\sqrt{2}}{2} \right) \quad (9)$$

where h_m , and σ are fitting parameters. While h_m (kPa) is a capillary pressure head, is related to the median pore radius, and σ , a dimensionless parameter, and a dimensionless parameter related to the pore radius distribution width. Substituting Equation (4) into Equation (9) provides Equation (10), Kosugi's volumetric water content log-normal distribution. The additional error function complicates log-normal distribution modeling. However, the model has greater flexibility in terms of representing the soil-water characteristic curve in the wet and dry regions for all soil types (Matlan *et al.*, 2014a).

Volumetric water content:

$$\theta = \theta_r + (\theta_s - \theta_r) Q \left[\frac{\ln\psi/h_m}{\sigma} \right] \quad (10)$$

Non-linear regression Analysis and Statistical Evaluation

Statistical analysis scores like R-square (R^2) and root mean square error (RMSE) were used to create a more accurate SWCC model and parameters. The values of R^2 indicate the model's fit to the experimental and fitted data sets (Habasimbi & Nishimura, 2019). On the other hand, the RMSE technique calculates the difference between the expected and actual values to evaluate the model's performance (Tao *et al.*, 2020). Previous studies have consistently shown that R^2 values close to 1 provide accurate numerical representations of the results, while RMSE near zero optimises model performance (Harisuseno & Cahya, 2020; Tao *et al.*, 2020; Esmaeelnejad *et al.*, 2015).

RESULT AND DISCUSSION

Physical Properties of the Garinono Formation

Table 1 presents the soil physical properties of the Garinono Formation, sampled at depths ranging from 1.5 m to 12.0 m below the ground surface. These properties include soil particle size distribution, specific gravity, field dry density, and natural moisture contents. The table illustrates that the soil samples predominantly consist of silt (45%–66%) and clay (16%–53%) particles. The soil in the research area is characterized by yellowish-brown and grey silty clay. Certain areas of the soil were notably dense and compact. Natural moisture concentrations ranged from low to high, making the

soil intermediate to low plastic, consistent with the findings of Musta *et al.* (2019) regarding Mélange soils.

Table 1. Summary of physical properties in the study area.

Sample Depth (m)	1.50 – 12.00
BS Classification	MI, ML, CI
Soil Description	Clayey SILT to Silty CLAY with traces of Gravel size stone fragments. Colour: Yellowish brown and grey.
Particle Size Distribution (%)	
Gravel (63 – 2 mm)	1 - 11
Sand (0.063 – 2 mm)	2 - 15
Silt (0.002 – 0.063 mm)	45 - 66
Clay (< 0.002 mm)	16 - 53
Atterberg Limit (%)	
Liquid Limit	30 - 40
Plastic Limit	12 - 22
Plastic Index	12 - 25
Specific Gravity	2.43 - 2.69
Field Dry Density (g/cm ³)	1.35 - 2.03
Natural Moisture Content (%)	4.78 - 39.45

Relationship between Soil Volumetric Water Content and Suction

Three (3) soil samples obtained at varying depths were examined utilizing a pressure plate extractor apparatus, encompassing a spectrum of suction values from 1 to 1500 kPa. Figure 2 illustrates the correlation between volumetric water content and suction (kPa), delineating the fluctuation of SWCC data across samples from distinct depths. As suction levels rise, there is a corresponding decrease in volumetric water content during the drying process. It is noteworthy that soil characteristics can exert a substantial influence on volumetric water content, even within limited geographical extents.

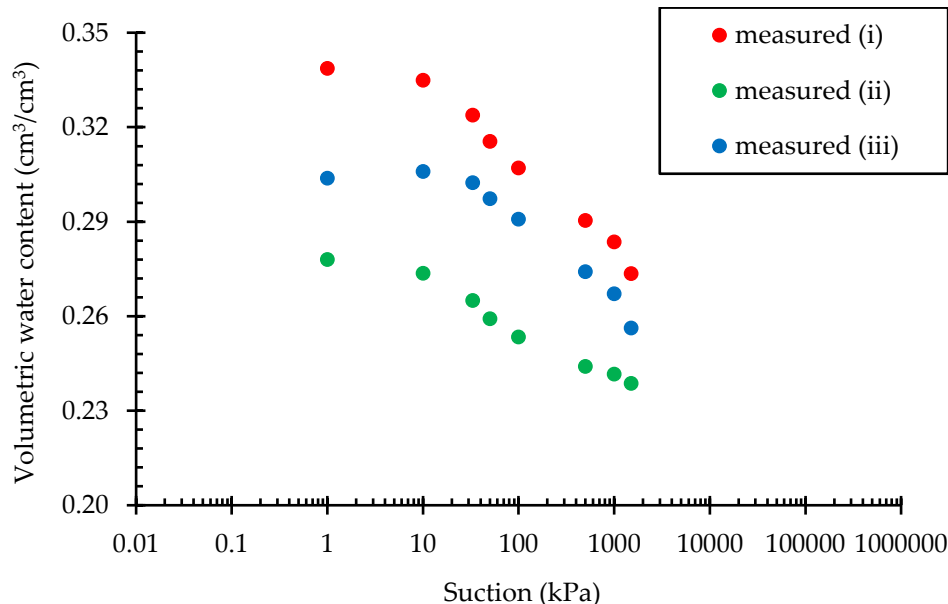


Figure 2. Relationship between measured volumetric water content and suction.

Notably, the study observed higher values of volumetric water content at high suctions, indicating that the soil samples retained moisture even at 1,500 kPa matric suction. This finding suggests that the silt clay soil from the Garinono Formation exhibits unsaturated conditions consistent with those of tropical clay soils, as previously reported by Oluyemi-Ayibiowu *et al.* (2020). Consequently, it

becomes necessary to apply higher suction values to extract water from the soil, given its unsaturated state, which encompasses the entire SWCC of the soil, as highlighted by Fondjo *et al.* (2020). Alternatively, empirical model fitting techniques can be employed to extrapolate the SWCC beyond the available data points, extending it toward higher suction values and providing a more comprehensive understanding of the soil's behavior.

Analysis of SWCC Parameters

Non-linear regression was employed to integrate SWCC model functions, and statistical indices R² and RMSE values were compared among four (4) different models: van Genuchten (1980) (VG), Fredlund & Xing (1994) (FX), Brooks & Corey (1964) (BC), and Kosugi (1994) (LN). This analysis aimed to enhance our understanding of the hydraulic behavior of soil samples from the Garinono Formation in Sandakan, Sabah.

Table 2 presents the fitted parameters for the Garinono soil samples collected, along with their bulk densities (BD or ρ_b) using the VG, FX, BC, and LN models, whereas Figure 3 illustrates SWCC fitting graphs for volumetric water measurements and the expected volumetric water content at different sample depths (i), (ii), and (iii).

Table 2. Bulk densities and model-fitted SWCC parameters of silt clay samples.

Soil parameter		van Genuchten (1980) model fitting					Statistical metrics	
Sample	ρ_b	θ_s	θ_r	α	n	m	R ²	RMSE
(i)	1.64	0.3404	0.1982	0.0609	1.1319	0.1165	0.9918	0.0020
(ii)	1.48	0.2782	0.2336	0.0552	1.4519	0.3112	0.9979	0.0006
(iii)	1.94	0.3057	1.00E-10	0.0123	1.0567	0.0537	0.9888	0.0019
Soil parameter		Fredlund and Xing (1994) model fitting					Statistical metrics	
Sample	ρ_b	θ_s	θ_r	a	n	m	R ²	RMSE
(i)	1.64	0.3402	0.0005	20.1090	1.0572	0.1343	0.9906	0.0022
(ii)	1.48	0.2780	0.1366	13.5540	1.6032	0.1577	0.9983	0.0006
(iii)	1.94	0.3061	1.78E-10	151.1500	0.8379	0.2082	0.9875	0.0062
Soil parameter		Brooks and Corey (1964) model fitting					Statistical metrics	
Sample	ρ_b	θ_s	θ_r	h_b	λ		R ²	RMSE
(i)	1.64	0.3387	1.00E-10	8.4644	0.0389		0.9929	0.0019
(ii)	1.48	0.2780	0.2093	6.9136	0.1565		0.9961	0.0009
(iii)	1.94	0.3048	2.28E-08	28.5020	0.0398		0.9875	0.0020
Soil parameter		Kosugi (1994) model fitting					Statistical metrics	
Sample	ρ_b	θ_s	θ_r	h_m	σ		R ²	RMSE
(i)	1.64	0.3412	0.2611	187.28	2.4124		0.9890	0.0024
(ii)	1.48	0.2786	0.2392	58.30	1.6351		0.9958	0.0009
(iii)	1.94	0.3057	0.2175	1193.00	2.3284		0.9886	0.0019

A nearly identical curve is observed in both saturated and partially saturated states when the models are fitted. Nevertheless, a discernible deviation emerges as the curve nears the unsaturated state. The observed inconsistency is hypothesized to be due to the scarcity of data concerning suction values more than 1,500 kPa. It is imperative to acknowledge that the capabilities of each SWCC model also exert an influence on this outcome.

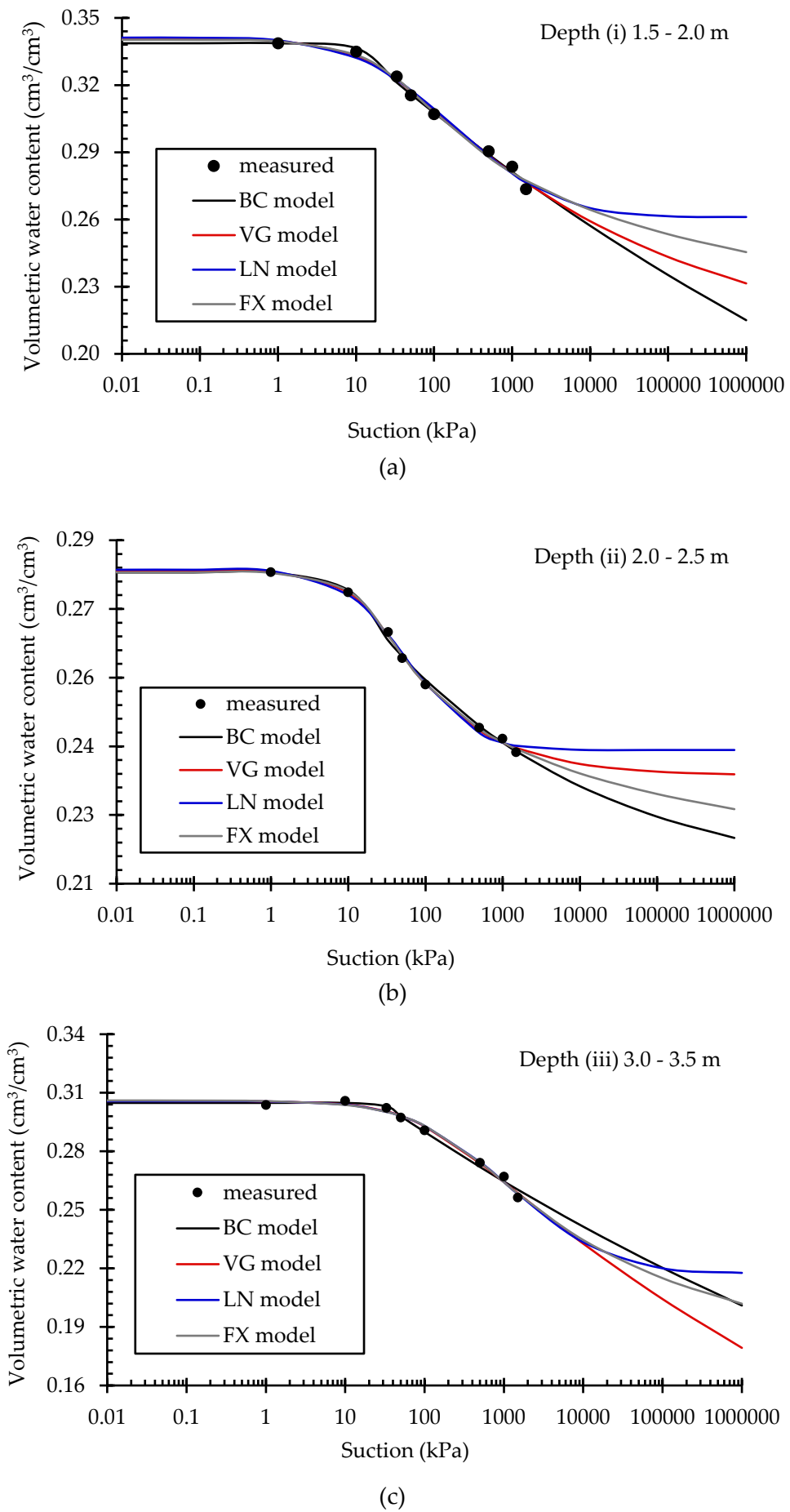


Figure 3. SWCC of three silt clay samples fitted with different empirical models.

The findings presented in Table 2 suggest that the R^2 values and RMSE ranges demonstrate satisfactory performance for all models in representing the SWCC of the Garinono Formation samples, based on the available measured dataset. However, the FX model stood out due to their ability to capture the complete spectrum of SWCC for the Garinono Formation. This was achieved through notably lower values of residual water content, θ_r , and a more comprehensive representation of SWCC toward higher suction values, distinguishing them from the other models.

The saturated volumetric water content, θ_s parameter displayed variations in values among the three soil samples (based on VG, FX, BC, and LN models), ranging from 0.2780 to 0.3412 cm^3/cm^3 , indicating the influence of distinct soil properties on its behavior. Moreover, all the models involved have two additional SWCC fitting parameters that are related to air entry values and pore size distributions. The results showed variations in each sample, emphasizing the impact of soil composition properties. Previous studies have shown that factors such as fine particle proportions, soil texture, structure, and clay mineralogy can influence initial volumetric water content and soil-water properties (Azmi *et al.*, 2019; Oluyemi-Ayibiowu & Akinleye, 2019; Osinubi & Bello, 2011; Song & Hong, 2020). Consequently, these variations contribute to the development of a unique SWCC for each sample. The fitting results for each model based on its own parameters reflect the outcomes of these findings (Table 2).

Effects of Bulk Density on SWCC

The effects of soil bulk density on SWCC behavior are prominently illustrated in Figure 4. Utilizing non-linear regression, the FX model accurately predicted values for silt clay samples from the Garinono Formation, showcasing how soils respond to fluctuations in water content under unsaturated conditions. The SWCC shape elucidates a soil's water retention capabilities across various suction values. Given the differing bulk densities of the soil samples, variations in θ_s and θ_r values are observed, offering insights into their water retention characteristics. Sample (i), characterized by a moderate bulk density, demonstrates commendable water-holding capacity when saturated, retaining some moisture even at high suctions. Conversely, sample (ii), with a lower bulk density, exhibits slightly diminished water retention when fully saturated but displays improved moisture retention during drying conditions. In contrast, sample (iii), featuring a higher bulk density, showcases intermediate θ_s values and experiences nearly complete moisture loss as the soil undergoes drying.

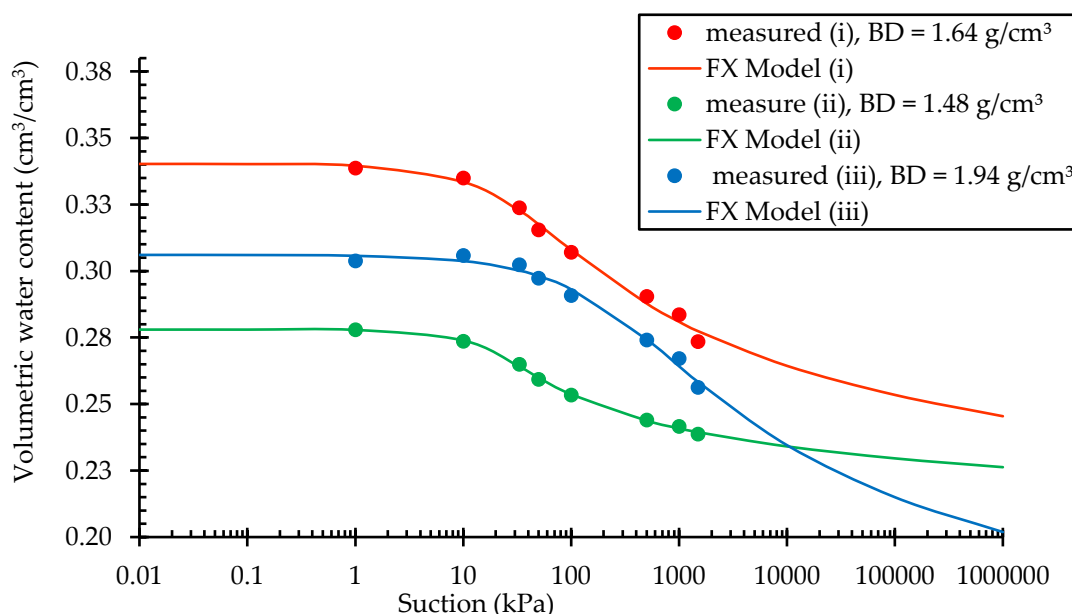


Figure 4. SWCC Variation with bulk density in Garinono Formation silt clay samples.

In soils with higher bulk density, such as sample (iii) with a bulk density of 1.94 g/cm^3 , the SWCC curve exhibits a steeper slope. This indicates that slight changes in levels result in larger changes in water content. Higher suction values are observed at the air entry value point in the SWCC curve for high bulk density samples. High-density soils release water faster during drying compared to lower density soils like samples (i) and (ii) with bulk densities of 1.64 g/cm^3 and 1.48 g/cm^3 , respectively. The steep SWCC curve in high bulk density soils indicates that water is released more easily as suction levels increase. This phenomenon is important for understanding how soil behaves when it is not saturated, as it impacts the availability and movement of water in the soil.

Soil composition and bulk density play crucial roles in water retention processes. Higher bulk density in soils leads to smaller pore spaces, posing challenges for water movement and retention, as noted by Zhao *et al.* (2022). Conversely, soils with lower bulk density exhibit larger pores and increased inter-particle spacing, enhancing their water retention capacity. Additionally, soil texture influences water retention dynamics. The findings suggest that samples with higher saturated water content, θ_s , generally exhibit higher VWC, with the concentration of clay in the soil often influencing this relationship, as observed by Fredlund & Xing (1994).

The bulk density (BD or ρ_b) of dry soil refers to its mass per unit volume, encompassing both solids and pores (Ray & Brady, 2017). This parameter plays a pivotal role in shaping various soil characteristics, including infiltration, water-holding capacity, and porosity. The size and distribution of soil pores, intricately linked to bulk density, significantly influence soil hydraulics, as highlighted by Majeti & Marcin (2020). Notably, soil bulk density exhibits an inverse relationship with soil porosity, with porosity decreasing as bulk density increases (Thomas & Klement, 2022). Figure 5 provides a visual comparison of soil porosity and bulk density. The sample at depth (iii) with a bulk density of 1.94 g/cm^3 displayed the lowest porosity values, followed by the sample at depth (i) with a bulk density of 1.64 g/cm^3 , while the sample at depth (ii) exhibited the highest porosity with a bulk density of 1.48 g/cm^3 . This finding underscores the impact of soil compaction on pore volume, reinforcing the inverse relationship between bulk density and soil porosity.

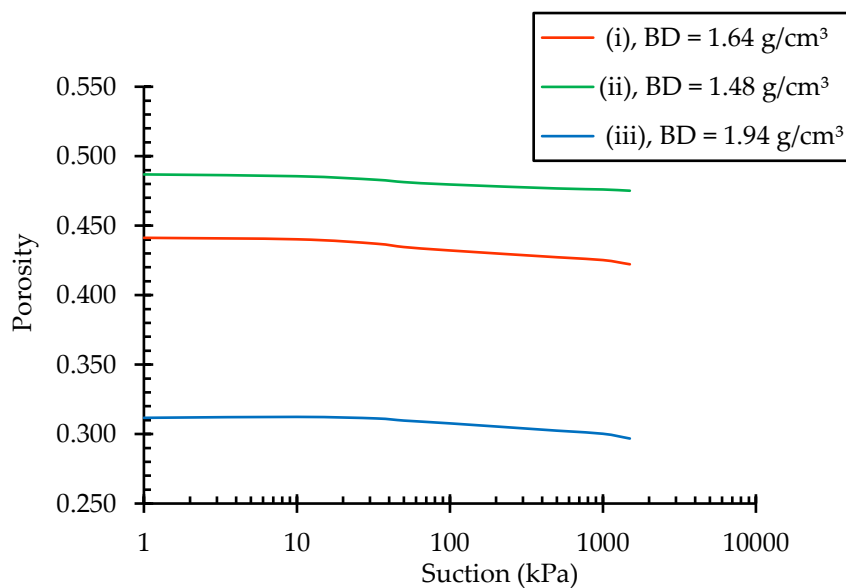


Figure 5. Relationship between porosity and bulk density in silt clay samples from the Garinono Formation.

CONCLUSION

Research conducted on the Garinono Formation has provided insights into its unsaturated behavior, highlighting the significance of soil-water characteristic curves (SWCC) in elucidating this transition. Among the models analyzed, the FX model emerges as the most accurate representation of SWCC data for the Garinono Formation soil, effectively capturing the entire spectrum of suction levels. SWCC offers valuable insights into how soil water content changes with varying suction levels, a phenomenon influenced by bulk density. Higher suction levels lead to decreased water retention and lower volumetric water content (VWC) values. Soils with higher bulk density tend to be more compacted, resulting in smaller pore spaces and a sharper decline in VWC. Conversely, soils with lower bulk density exhibit larger pore spaces, facilitating more efficient water retention.

The observed variations in SWCC hold significant implications across various applications. Soil samples with higher silt and clay content offer benefits in terms of water retention and stability, rendering them valuable for agricultural and drought-resilient purposes. However, it's essential to exercise caution with excessively saturated clay-rich soils to prevent issues such as swelling and structural damage. Striking a balance between the advantages of water retention and stability concerns is crucial when dealing with soil from the Garinono Formation.

ACKNOWLEDGEMENTS

The authors would like to express their appreciation for the financial support provided by Universiti Malaysia Sabah, Malaysia, through the GUG0577-1/2023 grant and the Ministry of Higher Education Malaysia through the RACER29-2019 grant.

REFERENCES

- [1] ASTM D2325-68. 2000. *Standard Test Method for Capillary-Moisture Relationships for Coarse- and Medium- Textured Soils by Porous-Plate Apparatus*. Annual Book of American Society for Testing and Materials (ASTM) Standards, 04(Reapproved), 1–6.
- [2] Azmi, M., Ramli, M. H., Hezmi, M. A., Mohd Yusoff, S. A. N. & Alel, M. N. A. 2019. Estimation of Soil Water Characteristic Curves (SWCC) of mining sand using soil suction modelling. *Institute of Physics Publishing (IOP) Conference Series: Materials Science and Engineering*, 527(2019), 012016.
- [3] Bello Yamusa, Y., Azril Hezmi, M., Ahmad, K., Anuar Kassim, K., Sa'Ari, R., Alias, N., Mustaffar, M., Kassim, A. & Rashid, A. S. A. 2019. Soil water characteristic curves for laterite soil at different water contents and methods as lining system. *Institute of Physics Publishing (IOP) Conference Series: Materials Science and Engineering*, 527(2019), 012002.
- [4] Brooks, R. H. & Corey, A. T. 1964. *Hydraulic Properties of Porous Media*. Colorado State University.
- [5] Cornelis, W. M., Khlosi, M., Hartmann, R., Van Meirvenne, M. & De Vos, B. 2005. Comparison of Unimodal Analytical Expressions for the Soil-Water Retention Curve. *Soil Science Society of America Journal*, 69(6), 1902–1911.
- [6] Ellithy, G. 2017. *A Spreadsheet for Estimating Soil Water Characteristic Curves (SWCC)*. ERDC/GSL TN-17-1. United State Army Corps of Engineers.
- [7] Esmaelnejad, L., Ramezanzpour, H., Seyedmohammadi, J. & Shabanpour, M. 2015. Selection of a suitable model for the prediction of soil water content in north of Iran. *Spanish Journal of Agricultural Research*, 13(1), 1–11.
- [8] European Standard. 1997. *Eurocode 7 - Geotechnical design - Part 2: Ground Investigation and Testing*. European Committee Standard.

- [9] Fashi, F. H., Gorji, M. & Shorafa, M. 2016. Estimation of soil hydraulic parameters for different land-uses. *Modelling Earth Systems and Environment*, 2(4), 1–7.
- [10] Fattah, M. Y., Al-Obaidi, A. A. & Al-Dorry, M. K. 2018. Determination of the Soil Water Characteristic Curve for Unsaturated Gypseous Soil from Model Tests. *Research Journal of Applied Sciences*, 13(9), 544–551.
- [11] Fondjo, A. A. & Dzogbewu, T. C. 2020. Swelling stress and suction correlation of compacted, heaving soils. *Civil Engineering and Architecture*, 8(4), 721–733.
- [12] Fondjo, A. A., Theron, E. & Ray, R. P. 2020. Investigation of the influencing soil parameters on the air entry values in soil-water characteristic curve of compacted heaving soils. *Civil Engineering and Architecture*, 9(1), 91–114.
- [13] Fredlund, D. G., Sheng, D. & Zhao, J. 2011. Estimation of soil suction from the soil-water characteristic curve. *Canadian Geotechnical Journal*, 48(2), 186–198.
- [14] Fredlund, D. G. & Xing, A. 1994. Equations for the soil-water characteristic curve. *Canadian Geotechnical Journal*, 31(4), 521–532.
- [15] Habasimbi, P. & Nishimura, T. 2019. Soil Water Characteristic Curve of an Unsaturated Soil under Low Matric Suction Ranges and Different Stress Conditions. *International Journal of Geosciences*, 10(01), 39–56.
- [16] Harisuseno, D. & Cahya, E. N. 2020. Determination of soil infiltration rate equation based on soil properties using multiple linear regression. *Journal of Water and Land Development*, 47(1), 77–88.
- [17] John, K. R. 2020. Swelling Clay Minerals and Slope Cut Failures in the Garinono Formation Along Jalan Sungai Hitam, Libaran, Sandakan. *Geological Behavior (GBR)*, 4(1), 29–34.
- [18] Khor, W. C., Chow, W. S. & Abd, H. A. R. 2015. Stratigraphic Succession and Depositional Framework of the Sandakan Formation, Sabah. *Sains Malaysiana*, 44(7), 931–940.
- [19] Kristo, C., Rahardjo, H. & Satyanaga, A. 2019. Effect of hysteresis on the stability of residual soil slope. *International Soil and Water Conservation Research*, 7(3), 226–238.
- [20] Leong, E. C. & Rahardjo, H. 1997. Review of Soil-Water Characteristic Curve Equations. *Journal of Geotechnical and Geoenvironmental Engineering*, 123(12), 1106–1117.
- [21] Luan, X. & Han, L. 2022. Variation Mechanism and Prediction of Soil–Water Characteristic Curve Parameters of Low-Liquid-Limit Silty Clay under Freeze–Thaw Cycles. *Applied Sciences*, 12(21), 10713.
- [22] Majeti, N. P. V. & Marcin, P. 2020. *Climate Change and Soil Interactions*. University of Hyderabad, Hyderabad, India. University of Agriculture in Krakow: Elsevier, Book Aid.
- [23] Mancuso, C., Jommi, C. & D’Onza, F. 2012. *Unsaturated Soils: Research and Applications Volume 2*. Heidelberg: Springer Berlin. pp. 437.
- [24] Matlan, S. J., Mukhlisin, M. & Taha, M. R. 2014a. Performance evaluation of four-parameter models of the soil-water characteristic curve. *The Scientific World Journal*, 2014, Article ID 569851.
- [25] Matlan, S. J., Mukhlisin, M. & Taha, M. R. 2014b. Statistical Assessment of Models for Determination of Soil Water Characteristic Curves of Sand Soils. *International Journal of Environmental, Ecological, Geological and Marine Engineering*, 8(12), 717–722.
- [26] Musta, B., Erfen, H. F. W. S., Karim, A. S. R., Kim, K. W. & Kim, J. H. 2019. Physico-chemical Properties and Mineralogical Identification of Soils from Mélange in Beluran-Sandakan, Sabah, Malaysia. *Journal of Physics: Conference Series*, 1358, 012073.
- [27] Okovido, J. O. & Obroku, E. O. 2021. Evaluation of Four SWCCs Models’ Flexibility for Selected Reconstituted Tropical Red Earth Soils. *The International Journal of Engineering and Science*, 10(2), 18–26.
- [28] Oluyemi-Ayibiowu, B. D., Akinleye, T. O., Fadugba, O. G. & Olowoselu, A. S. 2020. Soil-Water Characteristics of Tropical Clay Soil under High and Low Suction Conditions. *Journal of Geoscience and Environment Protection*, 08(11), 162–175.

- [29] Oluyemi-Ayibiowu, B. D. & Akinleye, T. O. 2019. Factors Influencing the Soil-Water Characteristics of Unsaturated Tropical Silty Sand. *Journal of Geoscience and Environment Protection*, 07(05), 264–273.
- [30] Osinubi, K. J. & Bello, A. A. 2011. Soil-Water characteristics curves for reddish brown tropical soil. *Electronic Journal of Geotechnical Engineering*, 16(2011), 1–25.
- [31] Ray, R. W. & Brady, N. C. 2017. *The Nature and Properties of Soils* (15th Edition). Upper Saddle River NJ: Pearson Press.
- [32] Roslee, R. 2018. Geohazards in Sandakan Town Area, Sabah, Malaysia. *Geological Behavior*, 2(1), 18–23.
- [33] Sharratt, B. S. 1990. *Water Retention, Bulk Density, Particle Size, and Thermal and Hydraulic conductivity of Arable Soils in Interior Alaska*. Bulletin 83, Agricultural and Forestry Experiment Station, School of Agriculture and Land Resources Management University of Alaska Fairbanks, October.
- [34] Song, Y. S. & Hong, S. 2020. Effect of clay minerals on the suction stress of unsaturated soils. *Engineering Geology*, 269, 105571.
- [35] Tao, G., Chen, Y., Xiao, H., Chen, Y. & Peng, W. 2020. Comparative Analysis of Soil-Water Characteristic Curve in Fractal and Empirical Models. *Advances in Materials Science and Engineering*, 2020, Article ID 1970314.
- [36] Thomas, M. & Klement, T. 2022. *Encyclopaedia of Inland Waters* (2nd Edition). Elsevier Inc.
- [37] van Genuchten, M. T. 1980. A Closed-form Equation for Predicting the Hydraulic Conductivity of Unsaturated Soils. *Soil Science Society of America Journal*, 44, 892–898.
- [38] Zhang, L., Li, J., Li, X., Zhang, J. & Zhu, H. 2018. *Rainfall-Induced Soil Slope Failure, Stability Analysis and Probabilistic Assessment*. Boca Raton: CRC Press.
- [39] Zhao, W., Zhou, C., Hu, J., Ma, F., & Wang, Z. 2022. Soil-Water Characteristic Curves and Fitting Models of Collapsible Loess: A Case Study of Lanzhou, China. *Polish Journal of Environmental Studies*, 31(4), 3455–3462.
- [40] Zou, L. & Leong, E. C. 2019. A simple method of estimating soil-water characteristic curve using point pedotransfer functions. *Japanese Geotechnical Society Special Publication*, 7(2), 287 - 292.